

Enhanced neuronal differentiation using plasma synthesized amino polymers

Estephanny Jocelyn Alvarado Muñoz, Roberto Olayo González, María Guadalupe Olayo González, Guillermo Jesús Cruz Cruz, Omar Eduardo Uribe Juárez, Angélica Coyoy Salgado, Daniel Martínez Fong, Hermelinda Salgado Ceballos, Carlos Enrique Orozco Barrios & Juan Morales Corona

To cite this article: Estephanny Jocelyn Alvarado Muñoz, Roberto Olayo González, María Guadalupe Olayo González, Guillermo Jesús Cruz Cruz, Omar Eduardo Uribe Juárez, Angélica Coyoy Salgado, Daniel Martínez Fong, Hermelinda Salgado Ceballos, Carlos Enrique Orozco Barrios & Juan Morales Corona (21 Mar 2024): Enhanced neuronal differentiation using plasma synthesized amino polymers, International Journal of Polymeric Materials and Polymeric Biomaterials, DOI: [10.1080/00914037.2024.2312824](https://doi.org/10.1080/00914037.2024.2312824)

To link to this article: <https://doi.org/10.1080/00914037.2024.2312824>



Published online: 21 Mar 2024.



Submit your article to this journal [↗](#)



Article views: 12




View related articles [↗](#)



View Crossmark data [↗](#)

Enhanced neuronal differentiation using plasma synthesized amino polymers

Estephanny Jocelyn Alvarado Muñoz^a, Roberto Olayo González^b , María Guadalupe Olayo González^c, Guillermo Jesús Cruz Cruz^c, Omar Eduardo Uribe Juárez^a, Angélica Coyoy Salgado^d, Daniel Martínez Fong^e, Hermelinda Salgado Ceballos^d, Carlos Enrique Orozco Barrios^d and Juan Morales Corona^b

^aDepartment of Electrical Engineering, Postgraduate Biomedical Engineering, Universidad Autónoma Metropolitana, Mexico City, México;

^bDepartment of Physics, Universidad Autónoma Metropolitana, Mexico City, Mexico; ^cDepartment of Physics, Instituto Nacional de Investigaciones Nucleares, Ocoyoacac, Mexico; ^dConacyt- Neurological Diseases Medical Research Unit, Instituto Mexicano del Seguro Social, Doctores, Mexico City, Mexico; ^eCenter for Research and Advanced Studies, of the National Polytechnic Institute, Mexico City, Mexico

ABSTRACT

Different pyrrole and allylamine polymeric materials, were synthesized by plasma polymerization with different powers and doped with iodine. The polymers were characterized physicochemically. A cell line of neuronal origin (N1E-115) was cultured on them to evaluate the effects of the materials on neuronal differentiation. Following a differentiation stimulus, immunofluorescence was performed, and the lengths of neurites, as well as the complexity of the network formed and the number of nuclei, were measured and analyzed to provide a differentiation index. The results showed that the polymeric materials exhibited different physicochemical characteristics depending on the synthesis conditions and enhanced neuronal differentiation.

ARTICLE HISTORY

Received 15 July 2023
Accepted 29 January 2024

KEYWORDS

Biopolymers; plasma polymerization; polypyrrole; polyallylamine

1. Introduction

Plasma-synthesized polymeric amino materials have been used as coatings, sensors, microfiltration membranes and enzyme electrodes and for protein immobilization and cell growth due to the chemical diversity of these molecules, and their hydrophilicities promote biocompatibility and adhesion in biological systems^[1-3]. These polymers have been used for these purposes because the primary and secondary amines are very polar due to the dipole moments of the electron lone pairs and the C-N and H-N bonds, and they can also form hydrogen (N-H) bridges. Protonated amines have localized positive charges in aqueous solutions at physiological pH (7.3), which can be used to interact with the negative charges of the cell and promote cell adhesion; this is why it is preferred to use polymers made from monomers containing amines, such as polyallylamine (PAL-I), which has a primary amine in the monomer, and polypyrrole (PPy-I), which has a secondary amine in the monomer.

Plasma-synthesized polymeric amine biomaterials change their physicochemical properties depending on the synthetic conditions used; these changes have been shown to influence cell adhesion and proliferation, but they may extend to other cellular processes (Table 1). These materials are commonly doped with a biocompatible electronegative element, usually iodine, to increase their electrical properties and generate semiconductors, which improves cell adhesion and proliferation^[4-8].

These plasma-synthesized amino polymers, specifically iodine-doped polypyrrole, have been used as implants in rat and monkey models with spinal cord injuries and show motor recovery in acute models of contusion injury and complete section injury^[9-10], and have also been shown to spare neural tissues and decrease cysts in these models^[11-14]. However, these characteristics do not explain the mechanisms for motor recovery in rats and monkeys, which is why it is necessary to study the effects of biomaterials in a more controlled model to evaluate the mechanisms for neuronal regeneration such as dendritic prolongation and cell differentiation.

It has been demonstrated that there are neurogenic niches in the spinal cord, such as in the ependymal canal and meninges, that have undifferentiated cells that can migrate to the affected site in case of a spinal cord injury, where the differentiate into the cell lineage required for repair of the injury^[15-18].

In this work, we present *in vitro* neuronal differentiation by plasma-synthesized amino polymers with the N1E-115 cell line.

2. Materials and methods

2.1. Syntheses of polymeric materials

The polymers were synthesized in a glass tubular reactor with a capacity of 1500 cm³; at each end, it has stainless steel flanges with two accesses each. Pyrrole (Sigma

Aldrich, $\geq 98\%$) and allylamine (Sigma Aldrich, 98%) monomers, as well as the iodine dopant (Sigma Aldrich, 98%), were connected to one of the flanges with the help of a “Y” wrench. A Pirani 945 MKS Instruments HPSTPM Products pressure gauge and a vacuum system consisting of a vacuum pump and a nitrogen trap that functioned as a condenser were connected to the other end. Two circular electrodes with diameters of 8 cm and at 10 cm from each other were placed inside the tube. The plasma polymerization reaction was initiated by connecting the electrodes to a Dressler CESAR-1500 radio frequency (RF) terminal, which generated an electromagnetic field of 13.56 MHz.

Cutout slides measuring 1×1 cm (Lauka, 26×76 mm) were placed inside the reactor, and the polymer films were deposited on them (Figure 1). Six syntheses were performed using the pyrrole and allylamine monomers, and synthetic powers of 20 W and 40 W were used to produce polypyrrole at 20 W (PPy-I 20 W), polypyrrole at 40 W (PPy-I 40 W), polyallylamine at 20 W (PAI-I 20 W), polyallylamine at 40 W (PAI-I 40 W), a copolymer at 20 W (PPy/PAI-I 20 W) and a copolymer at 40 W (PPy/PAI-I 40 W) (Table 1). After the polymerization was finished, the system was left to cool for

1 hour, and the reactor was opened to remove the coated coverslips for subsequent physicochemical characterization and cellular evaluation.

The hydrophilicities/hydrophobicities of the polymers were determined by performing contact angle measurements with distilled water and a Ramé-Hart Goniometer. The functional groups present in the polymeric materials were studied by attenuated total reflectance infrared spectroscopy (IR-ATR). The amine percentages of the polymers were determined by chemical derivatization with 4-trifluoromethyl benzaldehyde (TFBA) (Sigma Aldrich) for the primary amines and trifluoroacetic anhydride (TFAA) (Sigma Aldrich) for the secondary amines and -OH groups; the methodology of Ruiz et al. was used^[19], and the elemental atomic percentages before and after derivatization were determined by X-ray photoelectron spectroscopy (XPS).

Table 1. Polymer synthetic conditions.

Polymer	Polymerization time (minutes)	Power (W)	Pressure (Torr)
PPy-I	15	20, 40	$5.5 \times 10^{-1} \pm 1.1$
PAI-I	25	20, 40	$6.5 \times 10^{-1} \pm 1.4$
PPy/PAI-I	15	20, 40	$8.5 \times 10^{-1} \pm 1.4$

2.2. Cell culture

For the differentiation assay, the mouse neuroblastoma-derived cell Line N1E-115 (ATCC) was cultured; it was proliferated for 10 days in 75 cm² culture boxes (Corning) in Dulbecco's Modified Eagle Medium (DMEM) without pyruvate (Gibco), which was supplemented with 10% Fetal Bovine Serum (FBS) (Gibco), 1% Glutamax (Gibco) and 1% antibiotic (penicillin/streptomycin, Gibco). The culture medium was changed every 48 hours for 4 days and every 24 hours for the remaining days.

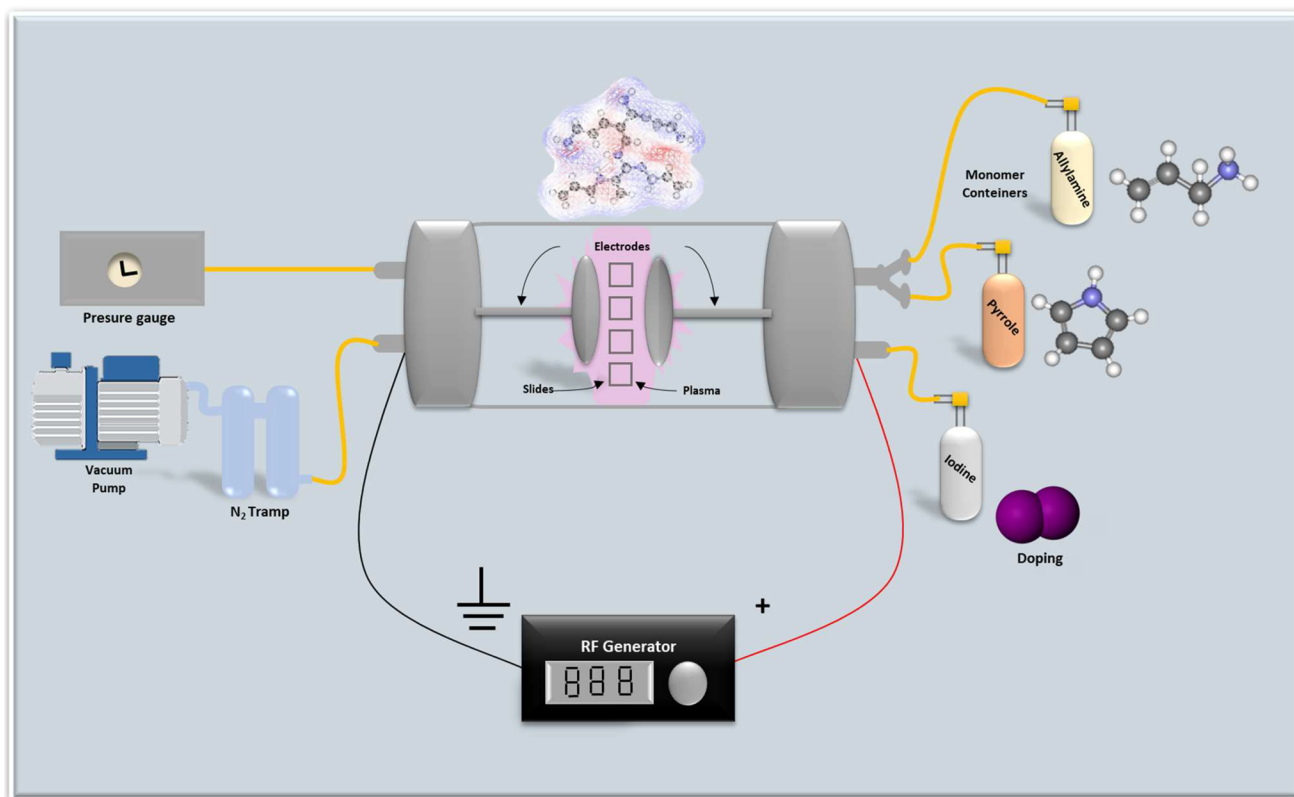


Figure 1. Plasma polymer syntheses.

2.3. Differentiation assays

The polymer films deposited on the slides were sterilized by ultraviolet light in a Stratagene Stratalinker 1800 UV Crosslinker for 30 minutes, and one material was placed in each well of a 24-well box. In each box, 3 slides without polymeric coatings were used as controls, and 3 slides were coated with each polymeric film (PPy-I, PAI-I and PPy/PAI-I) made with each synthetic power. Subsequently, 15,000 cells were seeded in each well. After 24 hours of seeding, the supplemented culture medium was removed and replaced with the differentiating medium, which consisted of DMEM, 1.25% Invitrogen brand dimethyl sulfoxide (DMSO), 2% SFB and 1% antibiotic, and this medium was used for 72 hours and changed at 48 hours. At the end of 72 hours in the differentiation medium, the cells were fixed with 4% paraformaldehyde (Sigma Aldrich) and washed with 1X PBS for 30 minutes for immunofluorescence determinations. Three independent experiments with this assay were performed for statistical purposes.

2.4. Immunofluorescence

For immunofluorescence labeling of the fixed cells, the 1X PBS in which they were immersed was removed, and they were permeabilized with 0.1% Triton (Sigma Aldrich) for 30 minutes. Then, in a humidity chamber, blocking of the nonspecific sites was carried out with 5% normal goat serum (Vector) for 30 minutes. Next, the primary antibody β III-Tubulin made in mouse (Abcam) was applied at a

concentration of 1:1000 for 12 hours at room temperature, and then the secondary antibody Alexa 488 anti-mouse (Molecular Probes) was applied at a concentration of 1:3000 and with an incubation time of 2 hours. The nuclei were counterstained with Molecular Probes Hoechst stain at a concentration of 1:1000. Between each step, washing was performed for 30 minutes with 1X PBS. Finally, the cells were embedded in Vectashield (Vector) and fixed on slides (Lauka, 26 \times 76 mm).

2.5. Measurement of neurite length and neuronal differentiation index

The dendritic extensions of the N1E-115 line seeded on the polymeric materials were observed with a Nikon confocal microscope, and the micrographs obtained using NIS-Elements software (Nikon) were analyzed with the NeuronJ plugin of the FIJI program, which allowed measurement of the lengths of the neuronal cell dendrites. The neurites of 25 cells were measured for each image.

To consider the number of dendrites and not only the lengths, a neuronal differentiation index was calculated by considering the complexity of the network and the number of nuclei for each network formed. For this, the micrographs were separated by channels using the Cell Profiler program to the green channel, and the area for the neuronal body of each micrograph was extracted from the blue channel (nuclei marked with DAPI) of the green channel (leaving only the neurites marked with -III Tubulin/Alexa 488) using the Cell

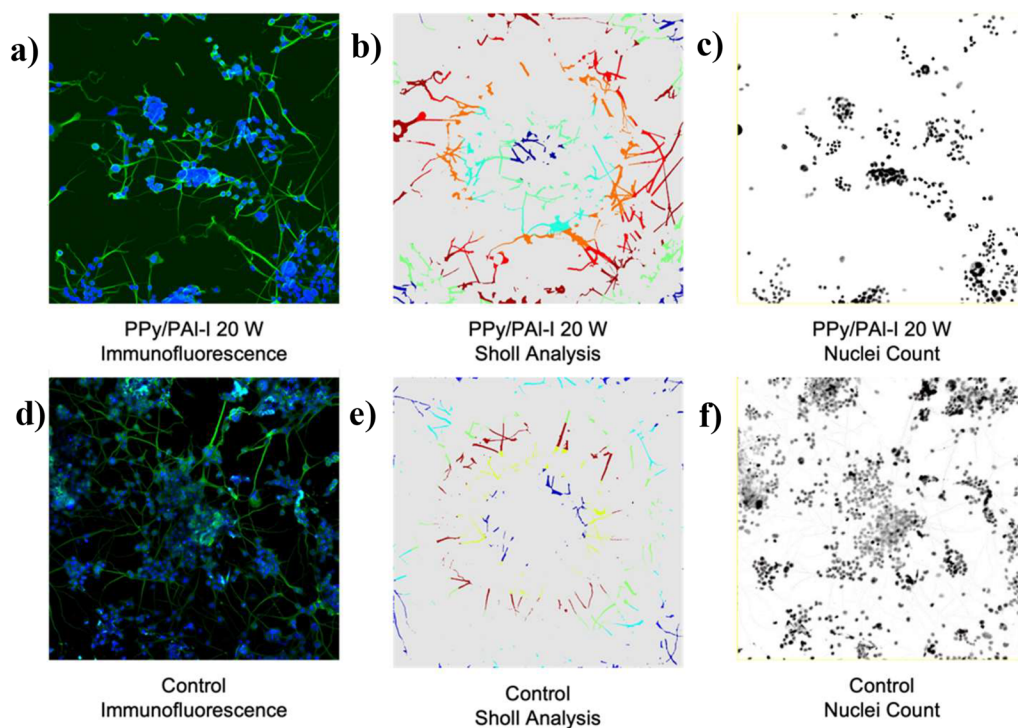


Figure 2. Image processing, Sholl analysis and nuclei count used to calculate the differentiation index. a) Micrograph of immunofluorescence of the neural network of N1E-115 trained on PPy/PAI-I 20 W, green: β -III-Tubulin, blue: DAPI, b) Sholl analysis mask of the neural network of N1E-115 trained on PPy/PAI-I 20 W, c) Nuclei count analysis mask of the neural network of N1E-115 trained on PPy/PAI-I 20 W, d) Micrograph of immunofluorescence of the neural network of N1E-115 trained on coverslips, green: β -III-Tubulin, blue: DAPI, e) Sholl analysis mask of the neural network of N1E-115 trained on coverslips, f) Nuclei count analysis mask of the neural network of N1E-115 trained on coverslips.

Profiler program (Figure 2a and d). Subsequently, the complexities of the neural networks formed on the materials (green channel) were analyzed using the FIJI program with the Sholl analysis tool, with which the sum of the crossings for each neurite with the concentric circles for each arc in the whole area of the neurites of each image was obtained (Figure 2b and e). Next, the number of nuclei in the blue channel of each image was counted with the ITCN plugin of the same FIJI program (Figure 2c and f). Finally, with the data obtained from each image, a differentiation index was determined as follows:

$$\frac{\text{No. Intersections (Sholl, green channel)}}{\text{No. Nucleus (Blue channel)}} = \text{Neural differentiation index}$$

A total of 15 micrographs were analyzed for each material and the control, and the statistics were performed using one-way ANOVA and Tukey's method for significant differences.

3. Results and discussion

3.1. Contact angles of the polymer films

The contact angles of the PPy-I polymers were 82.2°-87.6° for the polymer made at 20 W and 84.9°-84.1° for the polymer made at 40 W, while the contact angles of the PAI-I films were 77°-80.9° for the polymer made 20 W and 81.8°-83.8° for synthesis run at 40 W. For the copolymer films, the contact angles were 79°-82.4° for the polymer made 20 W and 87.7°-88.6° for the film synthesized at 40 W (Figure 3).

When the contact angle of the fluid on the surface of the material is close to 0°, it is classified as a superhydrophilic material; when it is less than 90°, it is a hydrophilic material; between 90° and 130°, it is considered hydrophobic; and at angles greater than 130°, it is considered superhydrophobic^[20]. According to this classification, all the synthesized materials were classified as hydrophilic materials. It is important to note that there was a trend indicating that the higher the synthetic power was, the greater the contact angles of the polymer films^[21]. Based on their ability to form hydrogen bridges with water (or their polarity), primary amines (NH₂) have contact angles of 43 ± 3°, and those of hydroxyl groups (OH) are 25 ± 3°^[22]. Therefore, it is suggested that films with lower contact angles, such as PAI-I 20 W, PPy/PAI-I 20 W, PPy-I 20 W and PAI-I 40 W, contained more hydrophilic functional groups, such as NH₂ and OH.

Several measurements were made with different volumes of water to confirm that coaxial or gravity forces did not influence the contact angles, which is why the angles varied at the beginning of the measurements and stabilized as the drop volumes increased. The variability and subsequent stabilization of the contact angle as the water droplet volume increased (PPy-I 20 W, PAI-I 20 W and PPy/PAI-I 20 W) indicated that the measurement results were not the products of coaxial forces or gravity.

3.2. Functional groups of the polymer films

ATR infrared spectroscopy over the range 4000 cm⁻¹ to 1250 cm⁻¹ was applied to PPy-I, PAI-I and PPy/PAI-I made at different synthetic powers (Figure 4). The bands at 3355 cm⁻¹ indicated the presence of N-H bonds

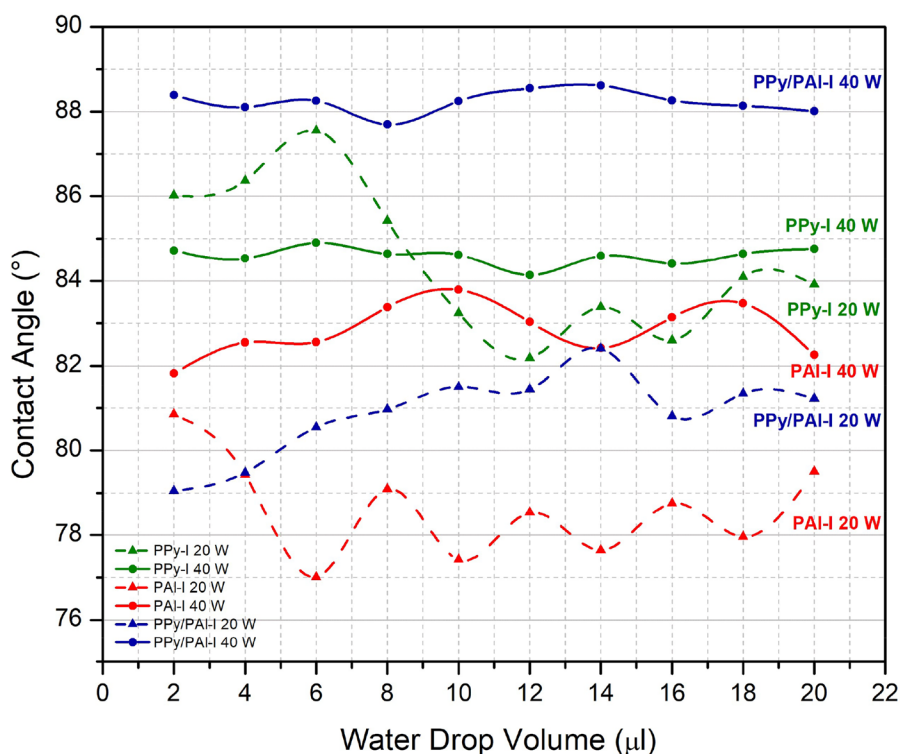


Figure 3. Polymer contact angles.

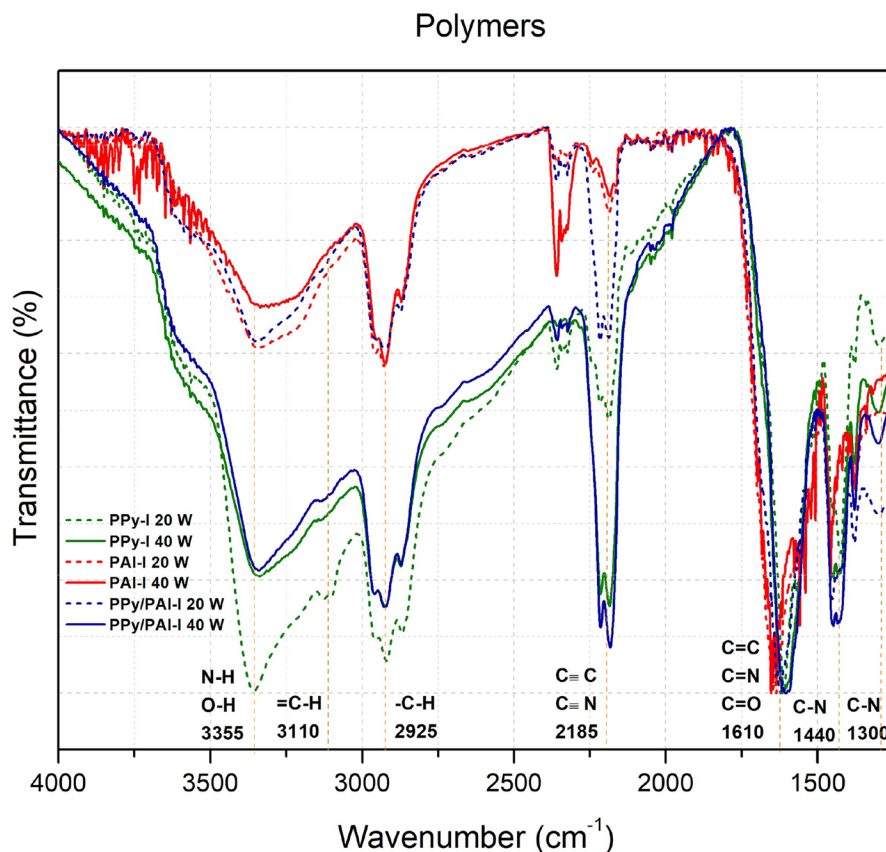


Figure 4. Polymer infrared spectra determined by ATR.

corresponding to the primary and secondary amines, imines and imides^[23,24] and were observed for all materials. The OH groups showed broad peaks in the IR spectra, which were observed to a greater extent in the PAI-I 20 W and 40 W coatings, as well as in the PPy/PAI-I 20 W coating; this coincided with the lower contact angles (Figure 3), suggesting there were more OH groups in these films. A peak at 3110 cm⁻¹ indicated the =C-H (conjugated) bonds of aliphatic structures, which were more defined in the PPy-I spectra due to the double bonds of the pyrrole monomer. Peaks at 2925 cm⁻¹ indicated aliphatic C-H bonds, which were present in greater proportions for the films synthesized at 40 W, suggesting rupture of the pyrrole rings and, in the case of PAI-I 40 W, greater substitution of the double bonds of the allylamine monomers. Bands were observed at 2185 cm⁻¹, which corresponded to unconjugated C≡C and N≡C triple bonded moieties^[23]; these were present in higher proportions in the PPy/PAI-I polymers and were found in higher proportions in the polymers synthesized at 40 W; in the spectra of the PAI-I polymers, this signal was weaker, suggesting that less dehydrogenation occurred during syntheses of the PAI-I films and more extensive dehydrogenation of the PPy-I and PPy/PAI-I polymers occurred at high powers. The bands at 1610 cm⁻¹ corresponded to C=C, C=N and C=O double bonds^[25]; these were the most intense signals for all of the materials, and they were stronger for both the PAI-I and PPy/PAI-I

20 W films, suggesting greater proportions of these groups in these films. The signals at 1440 cm⁻¹ and 1300 cm⁻¹ corresponded to the C-H and =C-H bonds of the pyrrole rings and were therefore not present in the spectra of the PAI-I films.

3.3. Percentages of amines and -OH groups in the polymeric films

It has been shown that the fluorine present in TFBA reacts selectively with primary amines via a specific reaction of the nitrogen with the carbonyl carbon of TFBA, and thus, elemental analyses with XPS made it possible to identify the fluorines reacting with the nitrogens of the primary amines and calculate the percentage of primary amines with respect to the carbon present in the molecule by using the following formula: ^[26-27]

$$\frac{[NH_2]_u}{[C]_u} = \frac{[F]_d[N]_u}{3[N]_d[C]_u} \times 100$$

where u represents the elements before derivatization and d represents the elements after derivatization. Chemical derivatization by TFAA has been used to estimate the percentages of primary and secondary amines present in materials; however, it has also been shown to react with -OH^[19,28,29], and the combined percentages of these functional groups can be calculated with the formula:^[19-23]

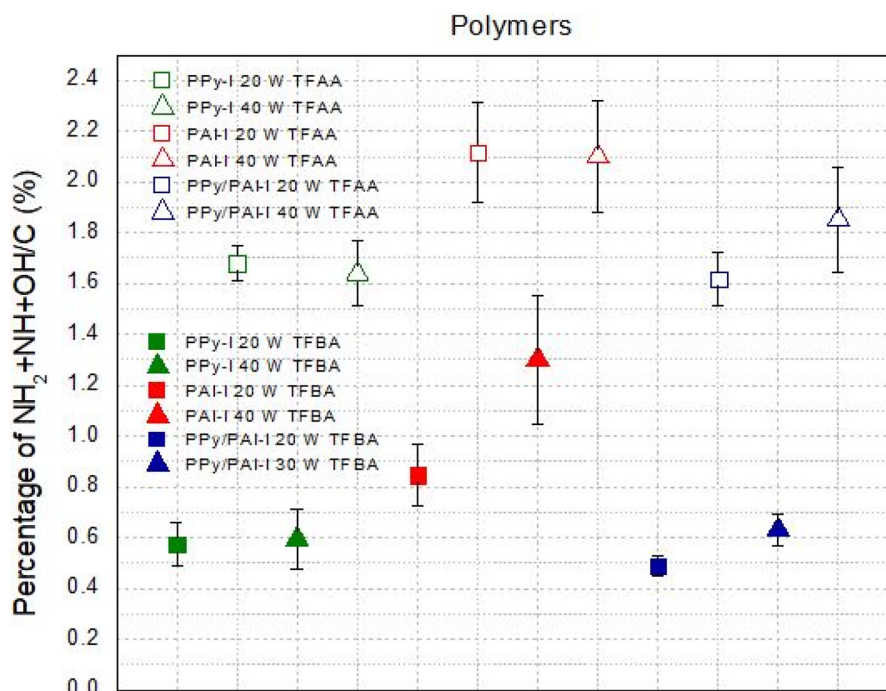


Figure 5. Percentages of NH₂, NH and OH functional groups determined by chemical derivatization with TFBA and TFAA.

Table 2. Polymer average elemental percentages before and after chemical derivatizations with TFBA and TFAA.

Polymers	Elemental compositions of polymers after and before derivatization											[NH ₂ +NH+OH]/[C](%) (TFBA)	[NH ₂ +NH+OH]/[C](%) (TFAA)
	Polymers			TFBA-Derivatized				TFAA-Derivatized					
	[C]%	[N]%	[O]%	[C]%	[N]%	[O]%	[F]%	[C]%	[N]%	[O]%	[F]%		
PPy-I 20W	83.4	11.8	4.8	76.0	11.0	8.0	1.3	83.2	9.2	3.5	4.1	0.57±0.09	1.68±0.07
PPy-I 40W	84.3	11.8	3.9	78.78	11.6	5.9	1.5	75.7	9.4	8.5	3.6	0.59±0.12	1.64±0.13
PAI-I 20W	83.2	12.2	4.3	72.2	11.5	9.3	2.0	75.9	10.8	7.3	4.6	0.85±0.12	2.12±0.20
PAI-I 40W	81.7	12.3	4.8	74.8	10.9	7.5	2.8	79.3	6.5	5.3	8.3	1.30±0.25	2.10±0.22
PPy/PAI-I 20W	85.0	11.1	3.5	79.3	11.5	5.4	1.3	76.8	9.3	6.6	5.2	0.49±0.04	1.62±0.11
PPy/PAI-I 40W	83.7	11.7	4.1	77.2	11.4	6.0	1.5	81.7	9.4	3.8	4.4	0.63±0.06	1.85±0.21

$$\frac{[NH_2 + NH + OH]u}{[C]u} = \frac{1/3[F]d}{[C]d - 2/3[F]d} \times 100$$

Figure 5 shows that the materials with the highest percentages of primary amines indicated by derivatization with TFBA were the PAI-I samples prepared at 20 and 40 W, which arose because the allylamine monomer has a primary amine in its structure; however, there were also primary amines in the PPy-I polymers in which the pyrrole monomer contained only a secondary amine. This was due to the nature of plasma polymerization, in which cross-linked polymers were generated by cleavage of the pyrrole rings and subsequent polymerization at different sites of monomers that were hydrogenated to form primary amines. The percentages of the -NH₂, -NH and -OH functional groups determined by TFAA were also higher for the PAI-I polymers, in which secondary amines were also formed by substitution during polymerization^[29].

Assuming accuracy of the derivatization experiments, the difference between the two derivatization processes (TFAA-TFBA) indicated the proportions of the -NH and

-OH groups. The PAI-I films are among the 3 polymers that showed a large difference between the two derivatives and therefore between the -NH and -OH groups (Table 2). The broad peak at 3355 cm⁻¹ and the high hydrophilicities of these 2 polymers suggested that the difference was mainly due to the presence of -OH groups.

3.4. Evaluation of neuronal differentiation of the N1E-115 line seeded on polymeric films

The N1E-115 cells adhered, proliferated, and differentiated on all materials, as shown in Figure 7. The average lengths of the dendritic extensions (Figure 6a) were 127 μm for the control, 241 μm for the PPy-I synthesized at 20 W and 203 μm for that synthesized at 40 W, 149 μm for the PAI-I synthesized at 20 W and 157 μm for that synthesized at 40 W and 137 μm for the PPy/PAI-I copolymer synthesized at 20 W and 126 μm for that synthesized at 40 W. In several studies using the neurite measurement technique, it was determined that the neuronal cell line was differentiated when the neurite lengths measured at least one diameter of

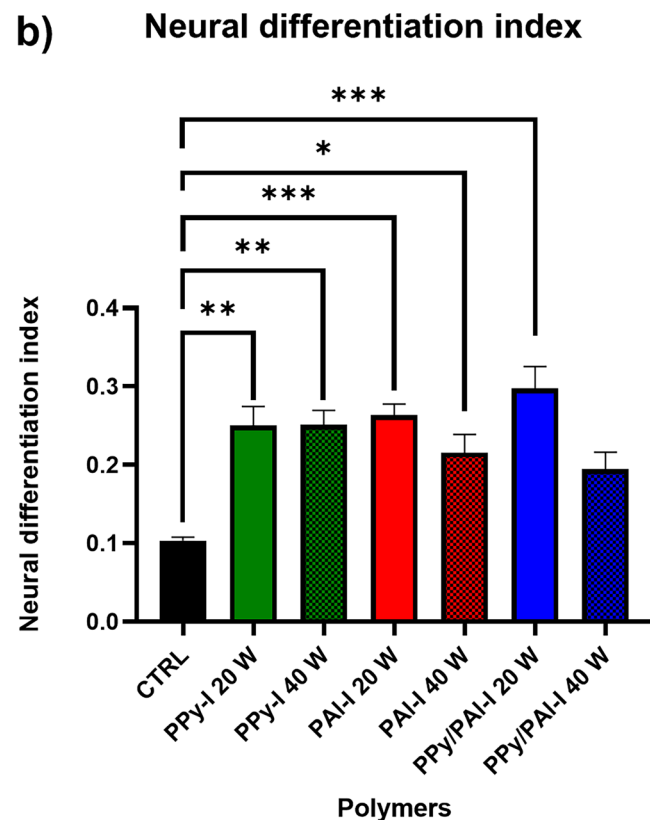
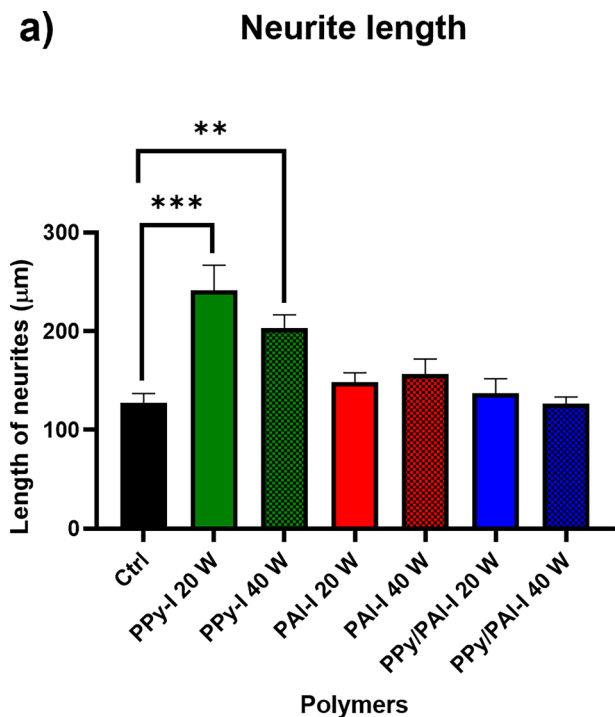


Figure 6. Analysis of N1E-115 neuronal networks formed on polymers. a) Neurite length plot, b) Neuronal differentiation index plot.

the cell body^[30,31]. In this case, cells seeded on all of the materials, including the control, were considered differentiated at 72 hours of treatment, as shown in Figure 7a–h, because the diameters of the core cell bodies averaged 22 µm; however, only cells seeded on the PPy-I polymers showed

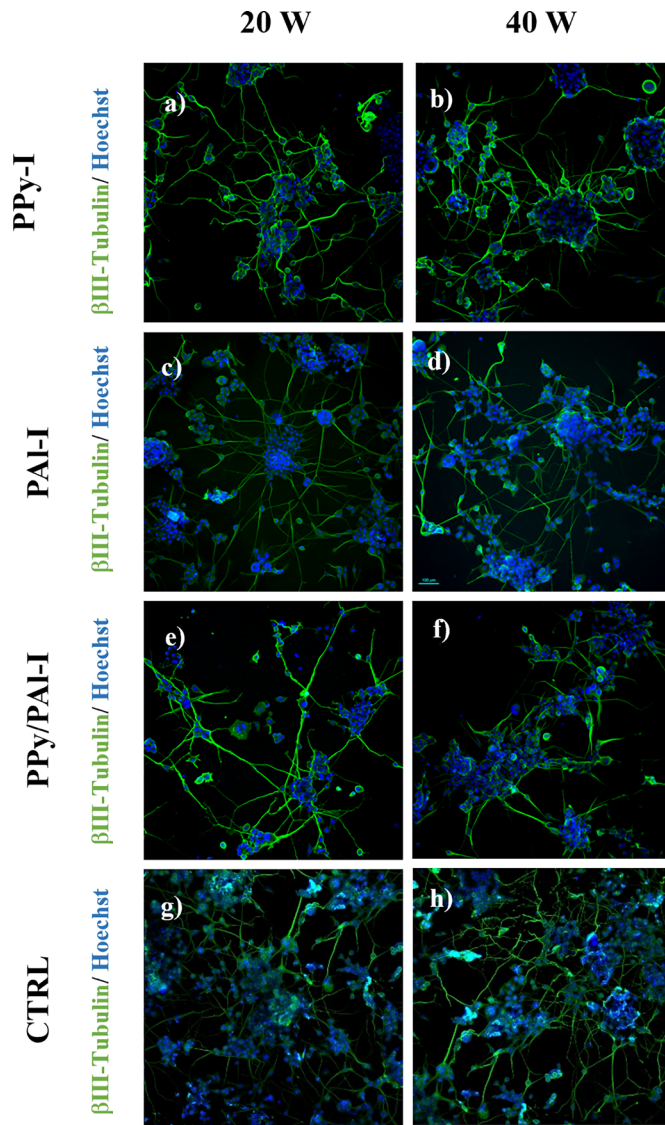


Figure 7. Immunofluorescence of the differentiated N1E-115 cell line on polymers, green: β III-Tubulin, blue: DAPI. a) PPy-I 20W, b) PPy-I 40W, c) PAI-I 20W, d) PAI-I 40W, e) PPy/PAI-I 20W, f) PPy/PAI-I 40W, g) Control 1, h) Control 2.

significant differences in dendritic length with respect to the control. The PPy-I polymers showed lower hydrophilicities and a lower percentages of primary and secondary amines based on both derivatizations; however, these were the polymers that showed the highest areas under the curves for the peaks at 3355cm^{-1} and 2185cm^{-1} in the IR-ATR spectra, suggesting that the functional groups present were the ones that affected the mechanism of dendritic prolongation in the N1E-115 cells and their differentiation. Because of their ability to form hydrogen bridges, it is suggested that the large contents of $-\text{NH}_2$, $-\text{NH}$ and $-\text{OH}$ groups indicated by the 3355cm^{-1} peak were mainly responsible for this effect.

Furthermore, it has been shown structurally that the p-rings present in the polymers are capable of forming π - π interactions between the π -orbitals of the electron-rich aromatic rings, such as those in the aromatic amino acids Phe, Tyr, Trp and Hys, and the electron-deficient PPy orbitals^[32]. Cation-type interactions have important roles in biological systems, and this type of bonding is important for

protein–protein interactions such as those that take place in enzymatic and ligand–receptor reactions^[33].

The electronic deficiency of the PPy molecule also enables the formation of interactions with anionic molecules such as the phosphate groups present in nucleic acids and cell membranes and the anionic amino acids Asp and Glu present in proteins^[34]. The ease with which PPy-I forms these noncovalent PPy/I bonds within biological systems and its high abundance at the end of synthesis suggested that it may have facilitated activation of the receptors or ion channels involved in dendritic elongation in the N1E-115 cell line.

The complexity of the network formed was analyzed with the method established by Sholl to analyze the dendritic branching patterns of neurons^[35]. Since the polymers arrested cell proliferation at earlier times than the control groups, there was a substantial difference in the number of cells present at the end of the study. For this reason, normalization of the cross-links in the dendritic network was performed with the concentric circles and the final numbers of cell nuclei. This normalization provides the differentiation index. The differentiation index based on the complexity of the neural network and the number of nuclei of the cells seeded on the materials (Figure 6b) was 0.10 for the control, 0.25 for the PPy-I made at 20 and 40 W, 0.26 and 0.22 for the PAI-I made at 20 W and 40 W; and 0.30 for the PPy/PAI-I copolymer made at 20 W, which was the material with the greatest significant difference relative to the control; the index and was 0.19 for the copolymer made at 40 W, which was the only material showing no significant difference with respect to the control. The differentiation indexes for most of the materials were significantly different from that of the control, except for that of the PPy/PAI-I 40 W copolymer; this also proved to be the least hydrophilic material, and it hindered cell adhesion and subsequent proliferation and affected cell differentiation. The PPy/PAI-I copolymer made at 20 W and the PAI-I made at 20 W showed the highest dendrite network complexities, and this seems to be more correlated with the hydrophilicities, since these 2 polymers showed the best wettabilities. On the other hand, these 2 polymers were among the 3 polymers with the greatest differences between derivatizations, as were PPy/PAI-I at 20 W and PAI-I at 20 W, which suggested a possible correlation with the percentages of secondary amines and -OH groups. Another association was shown between the differentiation index and the synthetic power.

The different effects exerted by the polymers suggested the possibility of different mechanisms for action. On the one hand, the polymers containing exclusively PPy/I (20 and 40 W PPy/I) favored neurite length and may have promoted axon reconnection across the lesion site. The polymers containing PAI-I (PAI-I 20 and PPy/PAI-I 20 W) showed the greatest significant differences for the complexity of the neuronal network, suggesting that they favored interconnections between the neurons, i.e., they may have favored synaptic plasticity, as demonstrated with the PPy-I polymer^[36].

4. Conclusions

The increases in synthetic power increased the contact angles and the hydrophilicities, and the increased power

raised the proportions of C≡N and C≡C groups and in turn increased the percentage of primary amines. All of the materials exhibited cell adhesion and proliferation, which reinforced the notion that materials polymerized by the plasma technique constitute good options for use as biomaterials in biomedical applications.

The plasma-synthesized amino polymers PPy-I, PAI-I and PPy/PAI-I contributed to enhanced neuronal differentiation of the N1E-115 cell line in different proportions depending on the synthetic powers and the monomers used, and a 20 W synthetic power was preferable in this context. Although there were certain trends in some variables that increased the effects on cell differentiation, it is also important to determine the different structural configurations that favor interactions with the molecules that effect differentiation.

Due to the effects of the materials mentioned previously, such as biocompatibility, adhesion and neuronal differentiation, these polymers could be used to repair central nervous system tissue, such as in spinal cord injuries for neuronal reconnection and increased neuronal plasticity.

It is recommended to continue with biological experimentation that reinforces the verification of the effect of neuronal differentiation as well as techniques that allow to establish specific metabolic pathways of differentiation that are activated by the treatment of these materials.

Acknowledgements

X-Ray Photoelectron Spectroscopy Technician, Ing. Rafael Basurto. Confocal Microscopy Technician, Dr. Vadim Pérez.

Disclosure statement

No potential conflict of interest was reported by the author(s).

Funding

This work was supported by CONACyT- 622686.

ORCID

Roberto Olayo González  <http://orcid.org/0000-0002-1728-958X>

References

- [1] Ardhaoui, M.; Bhatt, S.; Zheng, M.; Dowling, D.; Jolival, C.; Khonsari, y F. A. Biosensor Based on Laccase Immobilized on Plasma Polymerized Allylamine/Carbon Electrode. *Mater. Sci. Eng C Mater. Biol. Appl.* 2013, 33, 3197–3205. DOI: 10.1016/j.msec.2013.03.052.
- [2] Zuñiga-Aguilar, E.; Olayo, R.; Ramírez-Fernández, O.; Morales, J.; Godínez, y R. Nerve Cells Culture from Lumbar Spinal Cord on Surfaces Modified by Plasma Pyrrole Polymerization. *J. Biomater. Sci. Polym. Ed.* 2014, 25, 729–747. DOI: 10.1080/09205063.2014.898124.
- [3] Fabela-Sánchez, O.; Salgado-Ceballos, H.; Medina-Torres, L.; Álvarez-Mejía, L.; Sánchez-Torres, S.; Mondragón-Lozano, R.; Morales-Guadarrama, A.; Díaz-Ruiz, A.; Olayo, M.-G.; Cruz, G. J.; et al. Effect of the Combined Treatment of Albumin with

- Plasma Synthesised Pyrrole Polymers on Motor Recovery after Traumatic Spinal Cord Injury in Rats. *J. Mater. Sci. Mater. Med.* 2018, 29, 13. DOI: [10.1007/s10856-017-6016-2](https://doi.org/10.1007/s10856-017-6016-2).
- [4] Li, C.; Hsieh, J. H.; Lee, Y. T. Effects of Radio Frequency Power on the Microstructures and Properties of Plasma Polymerized Polypyrrole Thin Films. *Vacuum* 2017, 140, 132–138. DOI: [10.1016/j.vacuum.2016.09.009](https://doi.org/10.1016/j.vacuum.2016.09.009).
- [5] Wang, J.; Neoh, K. G.; Kang, Y. E. T. Comparative Study of Chemically Synthesized and Plasma Polymerized Pyrrole and Thiophene Thin Films. *Thin Solid Films* 2004, 446, 205–217. DOI: [10.1016/j.tsf.2003.09.074](https://doi.org/10.1016/j.tsf.2003.09.074).
- [6] Morales, J.; Olayo, M. G.; Cruz, G. J.; Castillo-Ortega, M. M.; Olayo, Y. R. Electronic Conductivity of Pyrrole and Aniline Thin Films Polymerized by Plasma. *J. Polym. Sci. B Polym. Phys* 2000, 38, 3247–3255. DOI: [10.1002/1099-0488\(20001215\)38:24<3247::AID-POLB60>3.0.CO;2-U](https://doi.org/10.1002/1099-0488(20001215)38:24<3247::AID-POLB60>3.0.CO;2-U).
- [7] Morales, J.; Olayo, M. G.; Cruz, G. J.; Olayo, Y. R. Synthesis by Plasma and Characterization of Bilayer Aniline-Pyrrole Thin Films Doped with Iodine. *J. Polym. Sci. B Polym. Phys.* 2002, 40, 1850–1856. DOI: [10.1002/polb.10254](https://doi.org/10.1002/polb.10254).
- [8] Arteshi, Y.; Aghanejad, A.; Davaran, S.; Omid, Y. Biocompatible and Electroconductive Polyaniline-Based Biomaterials for Electrical Stimulation. *Eur. Polym. J.* 2018, 108, 150–170. DOI: [10.1016/j.eurpolymj.2018.08.036](https://doi.org/10.1016/j.eurpolymj.2018.08.036).
- [9] Olayo, R.; Ríos, C.; Salgado-Ceballos, H.; Cruz, G. J.; Morales, J.; Olayo, M. G.; Alcaraz-Zubeldia, M.; Alvarez, A. L.; Mondragon, R.; Morales, A.; et al. Tissue Spinal Cord Response in Rats after Implants of Polypyrrole and Polyethylene Glycol Obtained by Plasma. *J. Mater. Sci. Mater. Med.* 2008, 19, 817–826. DOI: [10.1007/s10856-007-3080-z](https://doi.org/10.1007/s10856-007-3080-z).
- [10] Morales-Guadarrama, A.; et al. Spinal Cord Injury of Rhesus Monkey Implanted with PPy/I Plasma Polymer, MRI Study. Presented at the VI Latin American Congress on Biomedical Engineering CLAIB 2014, Paraná, Argentina 29, 30 & 31 October 2015. 2014, 174–177. DOI: [10.1007/978-3-319-13117-7_46](https://doi.org/10.1007/978-3-319-13117-7_46).
- [11] Cruz, G. J.; Mondragón-Lozano, R.; Diaz-Ruiz, A.; Manjarrez, J.; Olayo, R.; Salgado-Ceballos, H.; Olayo, M.-G.; Morales, J.; Alvarez-Mejía, L.; Morales, A.; et al. Plasma Polypyrrole Implants Recover Motor Function in Rats after Spinal Cord Transection. *J. Mater. Sci. Mater. Med.* 2012, 23, 2583–2592. DOI: [10.1007/s10856-012-4715-2](https://doi.org/10.1007/s10856-012-4715-2).
- [12] Morales-Guadarrama, A.; Salgado-Ceballos, H.; Morales, J.; Ríos, C.; Cruz, G. J.; Diaz-Ruiz, Y. A. CAT and MRI Studies of Spinal Cord Injured Rats Implanted with PPy/I. 2013, p. 12.
- [13] Alvarez-Mejía, L.; Morales, J.; Cruz, G. J.; Olayo, M.-G.; Olayo, R.; Díaz-Ruiz, A.; Ríos, C.; Mondragón-Lozano, R.; Sánchez-Torres, S.; Morales-Guadarrama, A.; et al. Functional Recovery in Spinal Cord Injured Rats Using Polypyrrole/Iodine Implants and Treadmill Training. *J. Mater. Sci. Mater. Med.* 2015, 26, 209. DOI: [10.1007/s10856-015-5541-0](https://doi.org/10.1007/s10856-015-5541-0).
- [14] Mondragon-Lozano, R.; Ríos, C.; Roldan-Valadez, E.; Cruz, G. J.; Olayo, M. G.; Olayo, R.; Salgado-Ceballos, H.; Morales, J.; Mendez-Armenta, M.; Alvarez-Mejía, L.; et al. Delayed Injection of Polypyrrole Doped with Iodine Particle Suspension after Spinal Cord Injury in Rats Improves Functional Recovery and Decreased Tissue Damage Evaluated by 3.0 Tesla in Vivo Magnetic Resonance Imaging. *Spine J.* 2017, 17, 562–573. DOI: [10.1016/j.spinee.2016.02.012](https://doi.org/10.1016/j.spinee.2016.02.012).
- [15] Decimo, I.; Bifari, F.; Rodriguez, F. J.; Malpeli, G.; Dolci, S.; Lavarini, V.; Pretto, S.; Vasquez, S.; Sciancalepore, M.; Montalbano, A.; et al. Nestin- and Doublecortin-Positive Cells Reside in Adult Spinal Cord Meninges and Participate in Injury-Induced Parenchymal Reaction. *Stem Cells* 2011, 29, 2062–2076. DOI: [10.1002/stem.766](https://doi.org/10.1002/stem.766).
- [16] Yang, L.; Li, G.; Ye, J.; Lu, D.; Chen, Z.; Xiang, A. P.; Jiang, M. H. Substance P Enhances Endogenous Neurogenesis to Improve Functional Recovery after Spinal Cord Injury. *Int. J. Biochem. Cell Biol.* 2017, 89, 110–119. DOI: [10.1016/j.biocel.2017.05.030](https://doi.org/10.1016/j.biocel.2017.05.030).
- [17] Moreno-Manzano, V. Ependymal Cells in the Spinal Cord as Neuronal Progenitors. *Curr. Opin. Pharmacol.* 2020, 50, 82–87. DOI: [10.1016/j.coph.2019.11.008](https://doi.org/10.1016/j.coph.2019.11.008).
- [18] Marichal, N.; García, G.; Radmilovich, M.; Trujillo-Cenóz, O.; Russo, R. E. Enigmatic Central Canal Contacting Cells: Immature Neurons in “Standby Mode”? *J. Neurosci.* 2009, 29, 10010–10024. DOI: [10.1523/JNEUROSCI.6183-08.2009](https://doi.org/10.1523/JNEUROSCI.6183-08.2009).
- [19] Ruiz, J.; Taheri, S.; Michelmore, A.; Robinson, D. E.; Short, R. D.; Vasilev, K.; Förch, R. Approaches to Quantify Amine Groups in the Presence of Hydroxyl Functional Groups in Plasma Polymerized Thin Films: Quantification of -OH in the Presence of -NH x Functional Groups in Amine Plasma Polymerized Coatings. *Plasma Processes Polym.* 2014, 11, 888–896. DOI: [10.1002/ppap.201400016](https://doi.org/10.1002/ppap.201400016).
- [20] Kota, A. K.; Kwon, G.; Tuteja, Y. A. The Design and Applications of Superomniphobic Surfaces. *NPG Asia Mater.* 2014, 6, e109–e109. DOI: [10.1038/am.2014.34](https://doi.org/10.1038/am.2014.34).
- [21] Agrawal, G.; Negi, Y. S.; Pradhan, S.; Dash, M.; Samal, Y. S. K. Wettability and Contact Angle of Polymeric Biomaterials. *Characterization Polymeric Biomater.* 2017, 57–81. DOI: [10.1016/B978-0-08-100737-2.00003-0](https://doi.org/10.1016/B978-0-08-100737-2.00003-0).
- [22] Keselowsky, B. G.; Collard, D. M.; García, Y. A. J. Surface Chemistry Modulates Fibronectin Conformation and Directs Integrin Binding and Specificity to Control Cell Adhesion: Surface Chemistry Alters Integrin Binding. *J. Biomed. Mater. Res. A* 2003, 66, 247–259. DOI: [10.1002/jbm.a.10537](https://doi.org/10.1002/jbm.a.10537).
- [23] Mangindaan, D.; Kuo, W.-H.; Chang, C.-C.; Wang, S.-L.; Liu, H.-C.; Wang, Y. M.-J. Plasma Polymerization of Amine-Containing Thin Films and the Studies on the Deposition Kinetics. *Surf. Coat. Technol.* 2011, 206, 1299–1306. DOI: [10.1016/j.surfcoat.2011.08.046](https://doi.org/10.1016/j.surfcoat.2011.08.046).
- [24] Eufinger, S.; van Ooij, W. J.; Ridgway, Y. T. H. DC Plasma-Polymerization of Pyrrole: Comparison of Films Formed on Anode and Cathode. *J. Appl. Polym. Sci.* 1996, 61, 1503–1514. DOI: [10.1002/\(SICI\)1097-4628\(19960829\)61:9<1503::AID-APP10>3.0.CO;2-R](https://doi.org/10.1002/(SICI)1097-4628(19960829)61:9<1503::AID-APP10>3.0.CO;2-R).
- [25] Cruz, G. J.; Gómez, L. M.; Gonzalez-Torres, M.; Gonzalez-Salgado, F.; Basurto, R.; Colín, E.; Palacios, J. C.; Olayo, M. G. Polymerization Mechanisms in Plasma Polyallylamine. *J. Mater. Sci.* 2017, 52, 1005–1013. DOI: [10.1007/s10853-016-0396-4](https://doi.org/10.1007/s10853-016-0396-4).
- [26] Ryssy, J.; Prioste-Amaral, E.; Assuncao, D. F. N.; Rogers, N.; Kirby, G. T. S.; Smith, L. E.; Michelmore, A. Chemical and Physical Processes in the Retention of Functional Groups in Plasma Polymers Studied by Plasma Phase Mass Spectroscopy. *Phys. Chem. Chem. Phys.* 2016, 18, 4496–4504. DOI: [10.1039/C5CP05850C](https://doi.org/10.1039/C5CP05850C).
- [27] Denis, L.; Cossement, D.; Godfroid, T.; Renaux, F.; Bittencourt, C.; Snyders, R.; Hecq, M. Synthesis of Allylamine Plasma Polymer Films: Correlation between Plasma Diagnostic and Film Characteristics. *Plasma Processes Polym.* 2009, 6, 199–208. DOI: [10.1002/ppap.200800137](https://doi.org/10.1002/ppap.200800137).
- [28] Siow, K. S.; Britcher, L.; Kumar, S.; Griesser, Y. H. J. Plasma Methods for the Generation of Chemically Reactive Surfaces for Biomolecule Immobilization and Cell Colonization - A Review. *Plasma Processes Polym.* 2006, 3, 392–418. DOI: [10.1002/ppap.200600021](https://doi.org/10.1002/ppap.200600021).
- [29] Friedrich, J.; Kühn, G.; Mix, R.; Unger, Y. W. Formation of Plasma Polymer Layers with Functional Groups of Different Type and Density at Polymer Surfaces and Their Interaction with Al Atoms. *Plasma Processes Polym.* 2004, 1, 28–50. DOI: [10.1002/ppap.200400008](https://doi.org/10.1002/ppap.200400008).
- [30] Hu, R.; Cao, Q.; Sun, Z.; Chen, J.; Zheng, Q.; Xiao, Y. F. A Novel Method of Neural Differentiation of PC12 Cells by Using Opti-MEM as a Basic Induction Medium. *Int. J. Mol. Med.* 2017, 41, 195–201. DOI: [10.3892/ijmm.2017.3195](https://doi.org/10.3892/ijmm.2017.3195).
- [31] Dwane, S.; Durack, E.; Kiely, Y. P. A. Optimising Parameters for the Differentiation of SH-SY5Y Cells to Study Cell Adhesion and Cell Migration. *BMC Res. Notes* 2013, 6, 366. DOI: [10.1186/1756-0500-6-366](https://doi.org/10.1186/1756-0500-6-366).
- [32] Mosch, H. L. K. S.; Höppener, S.; Paulus, R. M.; Schröter, B.; Schubert, U. S.; Ignaszak, Y. A. The Correlation of the Binding Mechanism of the Polypyrrole–Carbon Capacitive Interphase with Electrochemical Stability of the Composite Electrode. *Phys.*

- Chem. Chem. Phys.* 2015, 17, 13323–13332. DOI: [10.1039/C5CP01406A](https://doi.org/10.1039/C5CP01406A).
- [33] Lábás, A.; Krámos, B.; Bakó, I.; Oláh, y J. Accurate Modeling of Cation– π Interactions in Enzymes: A Case Study on the CDPCho:phosphocholine Cytidylyltransferase Complex. *Struct. Chem.* 2015, 26, 1411–1423. DOI: [10.1007/s11224-015-0658-9](https://doi.org/10.1007/s11224-015-0658-9).
- [34] Lucas, X.; Bauzá, A.; Frontera, A.; Quiñero, y D. A Thorough Anion– π Interaction Study in Biomolecules: On the Importance of Cooperativity Effects. *Chem. Sci.* 2016, 7, 1038–1050. DOI: [10.1039/C5SC01386K](https://doi.org/10.1039/C5SC01386K).
- [35] Sholl, D. A. Dendritic Organization in the Neurons of the Visual and Motor Cortices of the Cat.
- [36] Sánchez-Torres, S.; Díaz-Ruíz, A.; Ríos, C.; Olayo, M. G.; Cruz, G. J.; Olayo, R.; Morales, J.; Mondragón-Lozano, R.; Fabela-Sánchez, O.; Orozco-Barrios, C.; et al. Recovery of Motor Function after Traumatic Spinal Cord Injury by Using Plasma-Synthesized Polypyrrole/Iodine Application in Combination with a Mixed Rehabilitation Scheme. *J. Mater. Sci. Mater. Med.* 2020, 31, 58. DOI: [10.1007/s10856-020-06395-5](https://doi.org/10.1007/s10856-020-06395-5).